Available online at www.sciencedirect.com
SCIENCE DIRECT®
Optical Materials 28 (2006) 207–211
OPTICAL Materials
www.elsevier.com/locate/optmat

Growth and photorefractive properties of Zn, Fe double-doped $LiTaO_3$ crystal

Shuangquan Fang [a], Biao Wang [b,*], Tao Zhang [a], Furi Ling [a], Rui Wang [a]

[a] Electro-Optics Technology Center, Harbin Institute of Technology, P.O. Box 1225, Harbin 150001, China
[b] School of Physics and Engineering, Sun Yat-Sen University, Guangzhou 510275, China

Received 30 March 2004; accepted 28 December 2004
Available online 8 February 2005

Abstract

Zn, Fe double-doped $LiTaO_3$ crystals have been grown by the Czochralski method. The photorefractive properties and optical damage resistance were measured by the two-beam coupling experiments and transmitted facula distortion method, respectively. The results showed that the photorefractive response speed of Zn:Fe:$LiTaO_3$ was about four times faster than that of Fe:$LiTaO_3$, whereas the optical damage resistance was two orders of magnitude higher than that of Fe:$LiTaO_3$. In this paper, site occupation mechanism of impurities was also discussed to explain the high optical damage resistance and fast response speed of Zn:Fe:$LiTaO_3$ crystal.
© 2005 Elsevier B.V. All rights reserved.

Keywords: Zn:Fe:$LiTaO_3$ crystal; Exponential gain coefficient; Diffraction efficiency; Response speed; Optical damage resistance

1. Introduction

Lithium tantalate ($LiTaO_3$, LT) single crystal shows lots of properties similar to those of lithium niobate ($LiNbO_3$, LN) single crystal, such as the same crystalline structure (trigonal system, 3 m point cluster), ferroelectric in room temperature and Li deficiency, but its melting point (1650 °C) was higher that of LN (1240 °C). As one of the most excellent and useful photorefractive material, LT crystal can be applied in many areas, such as, surface acoustic wave (SAW) devices [1], waveguides devices [2], and holographic storage field [3]. Kim et al. [4] believed that the photorefractive effect of the crystals was attributed to the transition metal (TM) impurities and stacking faults caused by the nonstoichiometry and deficiency of oxygen in LT crystals, so it was an effective method to improve the photorefractive effect by doping the transition metal (TM) ions like Fe, Cu and Mn. Similar to that of LN, in TM-doped LT crystals, the photo-induced charge transport process can be described by

$$TM^{n+} \leftrightarrow TM^{(n+1)+} + e$$

where TM^{n+} (Fe^{2+}, Cu^{+} and Mn^{2+}) ions acted as electron donors and $TM^{(n+1)+}$ (Fe^{3+}, Cu^{2+} and Mn^{3+}) ions acted as electron traps. Charge carriers excited from TM^{n+} move until they are trapped by $TM^{(n+1)+}$, thus space charge fields build up and the refractive index is modulated because of the electro-optic effect. The bulk photogalvanic effect, as the main driving force of the space charges movement, has been identified. In Fe:LN and Fe:LT, the one-center scheme was experimentally verified, in which the bulk photogalvanic current density is proportional to light intensity and Fe^{2+} concentration [5]. Despite of excellent photorefractive properties, there were serious disadvantages in TM-doped LT, e.g. long response time and low optical damage resistance. The

* Corresponding author. Tel./fax: +860 2084115692.
E-mail address: wangbiao@hit.edu.cn (B. Wang).

0925-3467/$ - see front matter © 2005 Elsevier B.V. All rights reserved.
doi:10.1016/j.optmat.2004.12.011

so-called "optical damage" was also a photorefractive effect, which occurred when the crystals were irradiated with high-power laser beams of visible wavelengths. These effects limit its application in nonlinear optical fields.

It was well known that the optical damage resistance of LN crystals can be significantly improved by doping the optical damage resistance impurities such as Mg^{2+}, Zn^{2+}, In^{3+} and Sc^{3+} ions [6,7]. We also found that the optical damage resistance could be increased considerably when doping Zn^{2+} ions in Fe:LT crystals. In addition, the photorefractive response time of Zn:Fe:LT was reduced to a considerable degree in comparison with Fe:LT crystal.

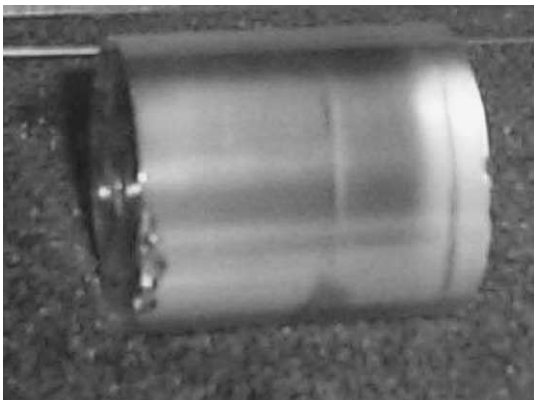

Fig. 1. As-grown boule of doubly-doped Zn:Fe:LT single crystal.

2. Crystal growth and specimen preparation

2.1. Crystal growth

Due to the high melting temperature of LT crystal, an intermediate frequency (IF) furnace was used to grow the LT crystals. For comparison with LT crystals, the LN crystals were also grown from the IF furnace by the Czochralski method. The starting materials used to grow the crystals were Li_2CO_3, Ta_2O_5, Nb_2O_5, Fe_2O_3 and ZnO, which were of all 4 N purity. Compositions of the raw materials were shown in Table 1. The crystals were grown at rotating rate 10–20 rpm and pulling rate 1–3 mm/h, and the axial temperature gradient of the IF furnace was 30–50 °C. After growth, the crystals were annealed to room temperature in air at the speed of 50 °C/h. The as-grown Zn:Fe:LT crystal was shown in Fig. 1.

2.2. Polarization of Zn:Fe:$LiTaO_3$ crystal

The Curie temperature of LT crystal, i.e. ferroelectric transition temperature, is 610 °C [8]. The crystal must be polarized to single-domain state before measurement. The following polarization technology was adopted: (1) The gold slurry was daubed on the c-sides of the crystals after cleaning, and they were heated to 350 °C in a muffle furnace. Then, the temperature was kept constant for 2 h to make the gold slurry reduced. (2) The crystals were heated to 750 °C to make the gold film that used as electrodes sintered. During the poling process, a DC electric field of 10–15 V/cm was applied at 700 °C, after 15 min the crystal was cooled down to room temperature at the rate of 40 °C/h. (3) Finally, the crystals that were polarized were cut into wafers and polished to optical grade. It was found by the etching experiments that the polarized crystals had single-domain structure.

Table 1
Composition of raw material and size of the samples

Crystal	Fe:$LiTaO_3$	Zn:Fe:$LiTaO_3$	Fe:$LiNbO_3$	Zn:Fe:$LiNbO_3$
[ZnO] (mol%)	0	7	0	7
[Fe_2O_3] (wt.%)	0.03	0.03	0.03	0.03
[Li]/[Ta] (mol ratio)	0.951	0.951	–	–
[Li]/[Nb] (mol ratio)	–	–	0.946	0.946
Wafer size ($a \times b \times c$, mm^3)	$5 \times 2 \times 5$	$5 \times 2 \times 5$	$10 \times 2 \times 10$	$10 \times 2 \times 10$

3. Photorefractive properties of Zn:Fe:$LiTaO_3$ crystals

3.1. Exponential gain coefficient

The photorefractive properties of the crystals were measured by the two-beam coupling experiments in the transmission geometry. Fig. 2 shows the typical experimental setup of the two-beam coupling. A weak probe wave (signal beam I_S) and a pump wave (reference beam I_R), which both originated from Ar^+ laser (wavelength $\lambda = 5145$ Å), irradiate on a sample with polarization direction parallel to the c-axis of the sample, then intensive beams coupling occurred and caused the signal beam intensity enhanced at the expense of the reference beam. The energy transformed from the pump beam to the signal beam can be evaluated by the exponential gain coefficient Γ, which can be described by the following equation [9,10].

$$\Gamma = \frac{1}{L} \ln \left(\frac{I_{ST}}{I'_{ST}} \cdot \frac{I'_{RT}}{I_{RT}} \right) \tag{1}$$

where I_{RT} (I'_{RT}) and I_{ST} (I'_{ST}) were the transmitted reference and signal beam intensity with (without) coupling, respectively; and L was the interaction length of the two beams in crystal. If $I'_{RT} \gg I'_{ST}$, the pump loss can be neglected, i.e., $I'_{RT} = I_{RT}$, thus Eq. (1) can be simplified as

$$\Gamma = \frac{1}{L} \ln \frac{I_{ST}\ (\text{with coupling})}{I'_{ST}\ (\text{without coupling})} \tag{2}$$

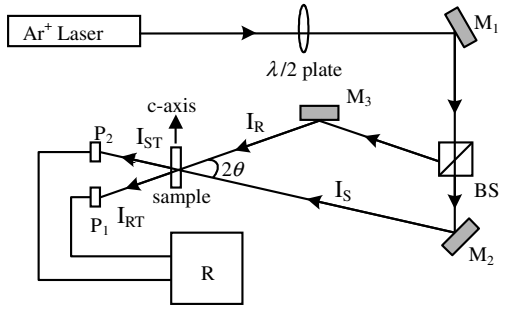

Fig. 2. Light path scheme of two-beam coupling experiment: M_1, M_2, M_3—mirrors; BS—beam splitters; P_1, P_2—photocells; R—recorder.

In this experiment, the diameters of the pump and signal beam were both 1 mm. The ratio of light intensity was $m = 1820$. The experimental results and fitting curve between the exponential gain coefficient Γ and 2θ were shown in Fig. 3, where θ was the half angle between the reference and signal beams. From the figure, one can find that the Zn:Fe:LT crystal had a maximal exponential gain coefficient (Γ_{max}) of 21.5 cm^{-1} at about the half angle of 9°.

3.2. Diffraction efficiency and response time

Diffraction efficiency and response time were also measured by the two-wave coupling experiment. Experimental setup is also shown in Fig. 2. Two coherent Ar^+ laser beams with identical intensity irradiate on the sample, in which the *c*-axis was oriented to be in the incident plane and perpendicular to the bisector of the two beams. The diffraction efficiency η was defined as the ratio between the diffractive and transmitting intensity, that is

$$\eta = I'_S/(I'_{ST} + I'_S) \times 100\% \quad (3)$$

where I'_{ST} was the transmitting intensity of I_S before the grating was established and I'_S was the diffractive intensity of I_S after the grating was established. The experimental results and fitting curve between the diffractive efficiency η and 2θ was given in Fig. 4, which indicates

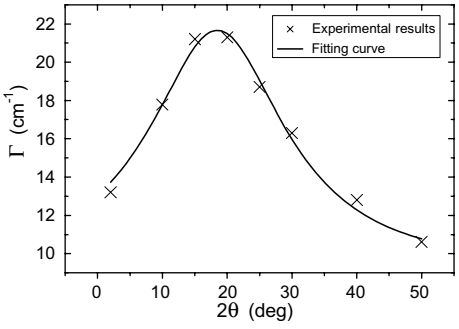

Fig. 3. The experimental results and fitting curve between exponential gain coefficient Γ and 2θ.

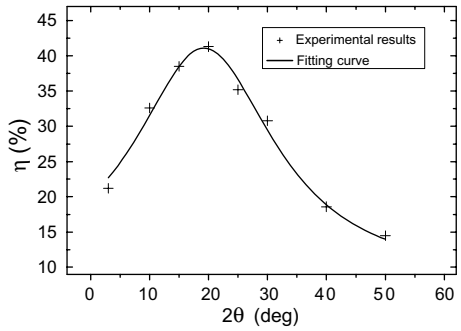

Fig. 4. The experimental results and fitting curve between diffractive efficiency η and 2θ.

that the diffractive efficiency of Zn:Fe:LT crystal will reach a maximum of 42% at about the half angle of 9.5°.

Response time τ was defined as the time interval from initial recording to the point when the diffraction efficiency reaches $\eta_{max}(1 - e^{-1})$, where η_{max} was the maximum value of the diffraction efficiency. The measured results were given in Table 2. In addition, the diffraction efficiency response curves for Fe:LT and Zn:Fe:LT crystals were also presented in Fig. 5 ($2\theta = 20°$).

4. Optical damage resistance of Zn:Fe:$LiTaO_3$ crystal

The optical damage resistance of Zn:Fe:$LiTaO_3$ crystal was evaluated by the transmitted facula distortion measurement. The experimental setup was shown in Fig. 6. An Ar^+ laser beam (wavelength $\lambda = 488$ nm),

Table 2
Photorefractive properties of the samples

Crystal	Fe:$LiTaO_3$	Zn:Fe:$LiTaO_3$	Fe:$LiNbO_3$	Zn:Fe:$LiNbO_3$
τ (s)	80	19	300	35
R (KW/cm^2)	1.32	328.6	0.54	61.7
η (%)	57	41	64	48
Δn (10^{-5})	6.54	5.32	7.09	5.85

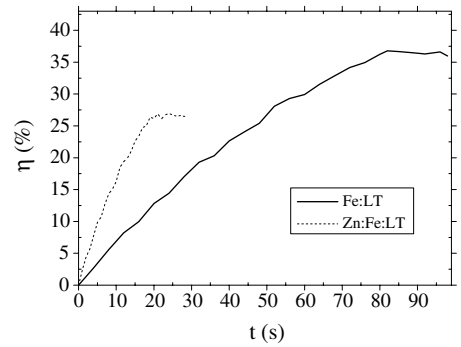

Fig. 5. Diffraction response curves of Fe:LT and Zn:Fe:LT crystals.

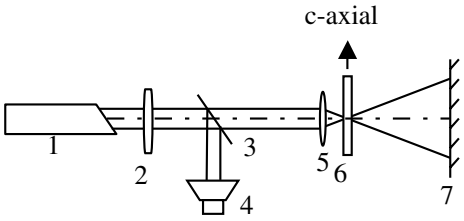

Fig. 6. Experimental setup of facula distortion measurement: 1, Ar^+ laser; 2, adjustable light attenuator; 3, beam splitter; 4, detector; 5, convex lens; 6, photorefractive crystal; 7, observation screen.

whose intensity can be controlled by an adjustable light attenuator and its polarizing direction was parallel to *c*-axis, irradiated on the samples after convergence through the convex lens. The crystal was placed on the focal plane of the lens.

The transmitted beam would not be distorted and the facula was still round under the low laser intensity. When the laser intensity reached a certain value, the transmitted facula would be smeared and elongated along the *c*-axis. The laser power density that just made the facula distorted was defined as the optical damage threshold *R* of the crystal. For comparison, the optical damage resistances of Fe:LT, Fe:LN and Zn:Fe:LN were also measured.

5. Results and discussion

The intensive light crawling effect that exists in thin Zn:Fe:LT samples may be responsible for the higher exponential gain coefficient in a large angle range, similar to that case in LN [11]. It can be found from Table 2 that the response speed of Zn:Fe:LT crystal was about four times higher than that of Fe:LT crystal and also higher than that of Zn:Fe:LN crystal. The optical damage resistance of all the samples were also given in Table 2, which indicated that the optical damage resistance of Zn:Fe:LT crystal was two orders of magnitude higher than that of Fe:LT crystal and was also higher than that of Zn:Fe:LN crystal. Using Kogelnik's formula [12]:

$$\eta = \sin^2\left(\frac{\pi L \Delta n}{\lambda \cos\theta}\right) \tag{4}$$

where the photorefractive index change Δn can be obtained from the experiment, thus the optical damage of these crystals can be evaluated quantitatively. The experimental setup was shown in Fig. 2. Two coherent Ar^+ laser beams with identical intensity were incident into the samples at $2\theta = 20°$ in the crystal. The experimental results were given in Table 2.

A well-known scalar expression can be used to explain the mechanism of the optical damage resistance increase in $LiTaO_3$ crystal [13], i.e., the photorefractive index change Δn can be expressed as

$$\Delta n = (n_e^3/2)\left[K j_{ph}(\sigma_{ph} + \sigma_d)\right] \tag{5}$$

where n_e is the extraordinary light refractive index, K is the electro-optic coefficient, j_{ph} is the photogalvanic current, σ_{ph} is the photoconductivity, and σ_d is the dark conductivity. σ_d can be neglected for $\sigma_d \ll \sigma_{ph}$ in our measurement, and the photogalvanic current is almost unchanged, so it is possible to reduce the optical damage by increasing only photoconductivity. Similar to that of the congruent LN crystal, the congruent LT crystal is also Li-deficient ([Li]/[Ta] < 1), therefore there are lots of intrinsic defects, such as anti-site tantalum (Ta_{Li}^{4+}) and lithium vacancy V_{Li}^{-} defects, in the LT crystal. In Fe:LT crystal, Fe^{3+} is the dominant electron acceptor, a reduced capture section of Fe^{3+} is responsible for the observed increase in photoconductivity. Ta_{Li}^{4+} is the most probable electron acceptor in the congruent LT host, so a reduced Ta_{Li}^{4+} concentration should also result in an increase of photoconductivity if the concentration of Fe^{3+} acceptor is negligible. There should be fewer intrinsic defects in the congruent LT than that in the congruent LN for [Li]/[Ta] > [Li]/[Nb]. In the congruent LN crystal, threshold concentration of ZnO is about 7 mol% [7], so the ZnO concentration should have exceeded its threshold in the congruent LT doping with 7 mol% ZnO in our samples. When doping Fe^{3+} in LT crystal, the role of Ta_{Li}^{4+} is negligible and Fe^{3+} will replace Ta_{Li}^{4+} and Ta^{5+} simultaneously, so photoconductivity is governed by the electron acceptor Fe^{3+}. Similar to the case in $LiNbO_3$ crystal [13], in Zn:Fe:LT crystal, Zn^{2+} takes the priority of replacing Ta_{Li}^{4+}, and Fe^{3+} will replace Ta_{Li}^{4+} and Ta^{5+} simultaneously. When the doped ZnO exceeds its threshold in Fe:LT crystal, all Ta_{Li}^{4+} were replaced completely, and Fe^{3+} only occupies Ta^{5+} sites. So the capture section of Fe^{3+} decreases significantly, which results in the photoconductivity increasing rapidly. Therefore Zn(7 mol%):Fe(0.03 wt.%):LT shows much higher optical damage resistance than that of Fe(0.03 wt.%):LT. Likewise, the increased photoconductivity by doping Zn^{2+} in Fe:LT crystal is also responsible for the fast response speed. Because the higher photoconductivity indicated that the motion of photo-induced charge carriers would become faster, which made the space charge field form faster, so photorefractive response speed was increased.

6. Conclusion

In conclusion, Zn:Fe:$LiTaO_3$ crystals were prepared by the Czochralski method and their photorefracive properties were measured. It was found that the photorefractive response speed can be greatly improved by doping ZnO in Fe:$LiTaO_3$ crystals, moreover, the optical damage resistance of Zn:Fe:$LiTaO_3$ was two orders of magnitude higher than that of Fe:$LiTaO_3$. Our analysis indicated that the increased photoconductivity was

responsible for both fast photorefractive response and high optical damage resistance in Zn:Fe:$LiTaO_3$ crystal.

Acknowledgments

This work was supported by the National Natural Science Foundation of China (50232030, 10172030), The National Science Foundation of Heilongjiang Province, The Ministry of Science and Technology of China through the High-Tech Program (2001AA31304), and the National Committee of Defense Science and Technology.

References

[1] A. Holm, Q. Stürzer, Y. Xu, R. Weigel, Microelectron. Eng. 31 (1996) 123.
[2] Ke-Ming Wang, Feng Chen, Hui Hu, Jian-Hua Zhang, Fei Lu, Bo-Rong Shi, Qing-Ming Lu, Chang-Qin Ma, Opt. Commun. 196 (2001) 215.
[3] Eckhard Krätzig, Karsten Buse, Top. Appl. Phys. 86 (2003) 23.
[4] B.K. Kim, G.Y. Kang, J.K. Yoon, J.H. Ro, J. Phys. Chem. Solids 61 (2000) 637.
[5] K. Buse, Appl. Phys. B 64 (1997) 391.
[6] Guoquan Zhang, Guangyin Zhang, Simin Liu, Guoyun Tian, Qian Sun, Opt. Lett. 22 (1997) 1667.
[7] T. Volk, N. Rubinina, M. Wöhlecke, J. Opt. Soc. Am. B 11 (1994) 1681.
[8] S.M. Kaczmarek, M. Swirkowicz, R. Jablonski, T. Lukasiewicz, M. Kwasny, J. Alloys Comp. 302 (2000) 204.
[9] Chunhui Yang, Yequan Zhao, Rui Wang, Minghua Li, Opt. Commun. 175 (2000) 247.
[10] Xuefeng Yue, S. Mendricks, Yi Hu, H. Hesse, D. Kip, J. Appl. Phys. 83 (1998) 3473.
[11] Jingwen Zhang, Wanjun Sun, Hua Zhao, Shaoping Bian, Kebin Xu, Minghua Li, Yuheng Xu, Opt. Lett. 18 (1993) 1391.
[12] H. Kogelnik, Bell Syst. Tech. J. 48 (1969) 2909.
[13] A.M. Glass, J. Electron. Mater. 4 (1975) 915.